



Fermi National Accelerator Laboratory

FERMILAB-FN-600

Use of a Shower Maximum Detector to Reduce Radiation Damage Sensitivity in EM Calorimetry

A. Beretvas, D. Green, J. Marraffino and W. Wu

*Fermi National Accelerator Laboratory
P.O. Box 500, Batavia, Illinois 60510*

December 1992

Disclaimer

This report was prepared as an account of work sponsored by an agency of the United States Government. Neither the United States Government nor any agency thereof, nor any of their employees, makes any warranty, express or implied, or assumes any legal liability or responsibility for the accuracy, completeness, or usefulness of any information, apparatus, product, or process disclosed, or represents that its use would not infringe privately owned rights. Reference herein to any specific commercial product, process, or service by trade name, trademark, manufacturer, or otherwise, does not necessarily constitute or imply its endorsement, recommendation, or favoring by the United States Government or any agency thereof. The views and opinions of authors expressed herein do not necessarily state or reflect those of the United States Government or any agency thereof.

FN – 600
December 19, 1992

Use of a Shower Maximum Detector to Reduce
Radiation Damage Sensitivity in EM Calorimetry

A. BERETVAS, D. GREEN, J. MARRAFFINO AND W. WU

Fermilab National Accelerator Laboratory

P. O. Box 500, Batavia, IL 60510

ABSTRACT

We construct a model for the effects of radiation damage on an electromagnetic calorimeter and use that model to investigate how a shower maximum detector might be used to monitor and partially compensate for that radiation damage.

Introduction

The design of the SDC electromagnetic calorimeter calls for the inclusion of a “shower max” detector consisting of one layer of rather finely segmented scintillator at some fixed depth in each calorimeter tower.¹ In contrast to all other scintillator tiles in the tower, whose light output is to be added together in a single phototube, the shower max detector will have a separate readout of its own. Completely aside from the physics motivation for including a device of this sort in the calorimeter design, the presence of a fully instrumented “extra” layer at a fixed depth in each tower provides an opportunity to use the information it provides in some interesting ways. This note is a description of one of them.

Several authors²⁻³ have pointed out that radiation damage is a major consideration for calorimetry at SSC energies. It is noted in Ref. 2 that longitudinal segmentation is one approach to dealing with the effects of radiation damage. Unfortunately, longitudinal segmentation is expensive and complex since even a simple two-fold segmentation doubles the number of readout channels. At the same time, an estimate of the accumulated radiation dose at SSC design luminosity in Ref. 3 shows that dose will range from 2.7 krad/year to 6.0 krad/year over the barrel region and increase to 600 krad/year in the most forward part of the endcap where $|\eta| = 3.0$. It is clear, then, that radiation damage represents a formidable problem, particularly for the endcaps of the SDC calorimeter.

In an attempt to make this problem somewhat more quantitative and to understand how the shower max detector might be used to mitigate it, we have made the Monte Carlo study described in the following sections. The particular emphasis here is on the issue of the effect of radiation damage on the energy resolution of the electromagnetic calorimeter. Recall that the fractional resolution is generally given by an expression of the form

$$\frac{\sigma}{E} = \frac{A}{\sqrt{E}} \oplus B \quad (1)$$

where the \oplus is used to indicate that the two terms are to be added *in quadrature*.

One of the design goals for the SDC electromagnetic calorimeter is to keep the “constant” term, B , less than 1%. Among other things, radiation damage will induce a B term which, not surprisingly, increases as the damage becomes more severe.

The Model

There are really only two aspects to the model we have used. The first is some representation of the effect of radiation damage on the detector and the second is a representation of how that damage would affect measured data. The basic tool for both is the SLAC program EGS4.⁴

Our representation of the radiation damage is based on assuming that the damage at any point in the calorimeter tower is linearly proportional to the time integrated energy deposit at that point. It follows from this that, within any given tower, the damage is fairly uniform in the transverse direction and has the shape of the energy deposit distribution in the longitudinal (z) direction. For any given geometry, that shape depends only on the energy spectrum of the particles producing the damage.

The geometry for our model tower follows that given in the SDC Technical Design Report¹ (TDR) for the endcap calorimeter. The tower consists of 100 alternating layers of 4 mm thick scintillating tiles and 6 mm thick lead absorbers, with the entire assembly positioned slightly more than 4 m from the intersection region. We have made our model tower substantially deeper than that specified in the TDR so as to minimize any leakage effects since they are not relevant to this study.

With the geometry fixed, the only remaining free parameter in our damage model is the energy spectrum of the damage-producing particles. For that, we have chosen electrons at a fixed energy of 10 GeV as being typical of $\eta = 3$ minimum bias neutral particles, presumably gammas from π^0 decay. The EGS4

program was used to generate 500 full showers for 10 GeV electrons. The longitudinal shape of the damage spectrum was then represented by the average energy deposit per tile over these 500 showers. Up to an overall normalization, this procedure completely fixes the model damage spectrum.

In addition to these 10 GeV showers, two more sets of higher energy showers were generated to represent data. Those consist of 450 showers produced by 150 GeV electrons and 400 showers produced by 250 GeV electrons. For each of these “data” showers, we have recorded the energy deposit per tile and the sum over all tiles. A histogram of these data for the 150 GeV showers revealed that the peak energy deposit occurs in tile 9 and we have chosen to fix the location of the shower max detector there. We denote that depth as z_{sm} . Since the position of maximum energy deposit varies roughly as $\ln(E)$, the damage profile, corresponding to 10 GeV showers, will peak at slightly smaller z and the energy deposit for the 250 GeV showers will peak at larger z .

Denoting the longitudinal energy deposition spectrum for the data showers as $E(z)$, and the longitudinal energy deposition spectrum for the damage showers as $D(z)$, we model the response of a damaged tower as

$$R(z; f) = E(z) - f N D(z) \tag{2}$$

where f is a number between 0 and 1 and will be referred to below as the damage fraction, and N is a normalization factor chosen so that $E(z)$ and $D(z)$ have equal intensity at $z = z_{sm}$. Defined in this way, $R(z_{sm}; f) = E(z_{sm})$ for $f = 0$ and $R(z_{sm}; f) = 0$ for $f = 1$. The physical interpretation of this is that the amount of light produced by each tile is reduced by an amount that is linearly proportional to the intensity of the damage spectrum, normalized to the data at $z = z_{sm}$. This means that f is the fractional light loss at shower maximum.

Application of the Model

A series of runs were performed over each of the 150 GeV and 250 GeV data sets varying f from 0.0 to 0.9 in steps of 0.1. Figure 1 shows the result for the 150 GeV data with $f = 0$. In the upper part of the figure, we have plotted the total energy deposit, E_d , on the vertical axis against the energy deposit in the shower max detector alone, E_{sm} , on the horizontal axis. As expected for $f = 0$, E_d does not depend on E_{sm} . The dotted line is a fit of the form

$$E_d = a + b E_{sm} \quad (3)$$

and the fact that $b = 0$ (within errors) verifies that E_d is independent of E_{sm} . In the lower part of the figure, we have plotted the projection of the scatter plot on the E_d axis and the residuals of the fit to the scatter plot. For this case, where $f = 0$, these histograms are essentially identical and the shower max detector has produced no new information. That changes for non-zero values of f as can be seen in Figs. 2 - 4 for the 150 GeV data and Figs. 5 - 8 for the 250 GeV data. There we see that, as f increases, E_d becomes more strongly dependent on E_{sm} . We can understand this by recalling that the shower max detector is at a fixed z in the tower. Because of that, its response measures how deeply a particle penetrates into the tower before showering begins. Since $D(z)$ has the shape of the energy deposition spectrum for relatively low energy particles, the damage is more severe at low z . Those particles which shower deep in the tower, producing a smaller signal in the shower max detector, are less affected by the damage than those which shower early in the most severely damaged part of the tower.

More to the point, we also see from the histograms in the lower portions of Figs. 2 - 4 that the simple projections of the data on the E_d axis become broader considerably faster than the residual distributions since the residual distributions take the correlation between E_d and E_{sm} into account while the simple projections do not. To measure the widths of these distributions in a consistent way,

we have fit each of these histograms to a gaussian and used the resulting σ as our estimator of the width. The values so obtained are shown in the inset to each of the histograms and summarized in Table 1 for the 150 GeV data and in Table 2 for the 250 GeV data. The columns labelled σ_p and E_p correspond to the simple projection histograms and those labelled σ_c and E_c correspond to the fit residual histograms. Note that, in contrast to the figures, the data in these tables have been renormalized to the full energy of the incident electron.

Before going on to discuss the effect on the energy resolution of our calorimeter, there is one more operational detail to describe. As can be seen from the total energy deposit histograms in Figs. 1 - 4, the mean energy deposit is dropping steadily as f increases. This does not correspond to how one operates a real calorimeter. A real calorimeter undergoes more-or-less continuous calibration designed to insure stable, reproducible and understandable data. One common aspect of that is to adjust gains so as to maintain a nearly constant relation between deposited energy and ADC channel number. So far, our model has not done that and is therefore somewhat unrealistic. There is a side effect of the usual energy calibration which, unless accounted for, could easily spoil our results. We have already noted that accumulated radiation damage reduces the output signal of a calorimeter. Then, to keep the response constant for some fixed energy deposit, it is always necessary to *increase* the gain. Doing that to some distribution does indeed move the mean as intended but it also necessarily *increases* the width. This procedure makes the real effect of radiation damage on the detector apparent. To account for the full effect of this detector calibration, we have rescaled the detector response as defined by Eq. (2) for all $f > 0$ to the same mean value as that for the $f = 0$ case. Figs. 9 - 11 show the 150 GeV data after rescaling and Figs. 12 - 14 show the 250 GeV data after rescaling. The results obtained in this way are summarized in Table 3 for the 150 GeV data and Table 4 for the 250 GeV data. Just as for Tables 1 and 2, the data in these tables have been renormalized to the full energy of the incident electron.

For all four tables, the values of A and B were calculated as follows. For each

set of data, we assume that $B = 0$ for $f = 0$. Then

$$A = \frac{\sigma(f = 0)}{\sqrt{E(f = 0)}} \quad (4)$$

or

$$A = \frac{\sigma_0}{\sqrt{E_0}} \quad (5)$$

We then take this value of A as fixed for all other values of f in the data set. For the 150 GeV data, $A = 0.152$ and for the 250 GeV data, $A = 0.155$. We obtain the induced constant term as a function of f by substituting this expression for A into Eq. (1). Rearranging the terms yields

$$B = \frac{\sqrt{\sigma_i^2 - \sigma_0^2}}{E_i}, \quad i = 1, 9 \quad (6)$$

There are two possible values for B , one labelled B_p corresponding to σ_p and E_p and the other labelled B_c corresponding to σ_c and E_c .

Recall that our purpose is to see if we could tolerate a higher radiation dose and still limit B to no more than 1%. Concentrating on the renormalized data, we see that the answer is yes. For the 150 GeV data, (See Table 3.) B_p has reached 1% for f slightly greater than 0.1 whereas B_c remains less than 1% until f is almost 0.2. For the 250 GeV data, (See Table 4.) B_p has reached 1% for $f \approx 0.15$, while B_c does not reach that value until $f \approx 0.22$. The variation of B_p and B_c as functions of f is summarized in Fig. 15 for the 150 GeV data and Fig. 16 for the 250 GeV data. That the resolution for higher energy particles is less seriously affected follows because higher energy particles tend to penetrate more deeply into the tower where the damage is less severe.

To put our results into perspective, we can make a rough estimate of the radiation dose required to produce a particular damage fraction and, from that, estimate the lifetime of the scintillator. In Ref. 3, it is shown that the normalized response of a typical scintillator to a dose, D , is roughly given by $r = \exp(-D/D_0)$

where D_0 is a characteristic of the scintillator. For SCSN81/BCF91, $D_0 \approx 3.6$ Mrad. Interpolating in Table 1, we see that the renormalized energy deposit for $f = 0$ is 150 GeV (by definition), that for $f = 0.12$, where B_p is 1%, is 137.5 GeV, and that for $f = 0.19$, where B_c is 1%, is 130.4 GeV. The normalized response at $f = 0.12$ is $137.5/150.0 = 0.92$ which corresponds to $D = 0.3$ Mrad. Similarly, the normalized response at $f = 0.19$ is $130.4/150.0 = 0.87$ which corresponds to $D = 0.5$ Mrad. For the worst case mentioned earlier of 0.6 Mrad/year, these values of D would require 6 months and 10 months respectively. The same calculation using Table 2 for the 250 GeV case, yields $D = 0.4$ Mrad when B_p is 1% and $D = 0.6$ Mrad when B_c is 1%. Again at 0.6 Mrad/year, accumulating these values of D would require 8 months and 1 year respectively. Thus, in both cases, we have bought a factor of about 2 of detector operation before the most severely damaged scintillator would have to be replaced. This is similar to the results found previously in Refs. 2 and 3 using longitudinal segmentation.

REFERENCES

1. SDC Technical Design Report, SDC-92-201, 1 April 1992.
2. D. Green, A. Para and J. Hauptman, Radiation Damage, Calibration and Depth Segmentation in Calorimeters, FERMILAB FN-565, May 1991.
3. D. Green, Calorimetry and Radiation Damage, FERMILAB FN-583, June 1992.
4. W. R. Nelson, Hideo Hirayama and David W. O. Rogers, The EGS4 Code System, SLAC-265, Dec. 1985.

f	σ_p	E_p	B_p	σ_c	E_c	B_c
0.0	1.86	150.0	0.000	1.91	150.0	0.000
0.1	2.08	139.4	0.007	1.86	139.4	0.000
0.2	2.71	128.7	0.015	2.10	128.8	0.007
0.3	3.34	118.0	0.024	2.50	118.1	0.014
0.4	4.39	107.2	0.037	2.96	107.5	0.021
0.5	5.21	96.4	0.051	3.72	96.9	0.033
0.6	6.14	85.7	0.068	3.94	86.3	0.040
0.7	7.21	75.0	0.093	4.27	75.7	0.050
0.8	8.11	68.0	0.116	5.16	65.2	0.074
0.9	8.38	57.5	0.142	5.18	58.3	0.083

Table 1. 150.0 GeV Incident Electrons - Unnormalized Data

f	σ_p	E_p	B_p	σ_c	E_c	B_c
0.0	2.46	250.0	0.000	2.39	250.0	0.000
0.1	2.75	233.1	0.005	2.33	233.2	0.000
0.2	3.99	216.2	0.015	2.92	216.6	0.008
0.3	4.95	199.0	0.022	3.05	199.9	0.010
0.4	6.79	182.8	0.035	3.71	183.2	0.016
0.5	8.12	166.3	0.047	4.46	166.6	0.023
0.6	9.91	149.1	0.064	5.27	149.9	0.031
0.7	11.31	132.6	0.083	6.03	133.4	0.042
0.8	12.56	115.5	0.107	6.60	117.0	0.053
0.9	17.43	99.2	0.174	6.63	105.7	0.059

Table 2. 250.0 GeV Incident Electrons - Unnormalized Data

f	σ_p	E_p	B_p	σ_c	E_c	B_c
0.0	1.86	150.0	0.000	1.91	150.0	0.000
0.1	2.22	150.0	0.008	2.02	150.0	0.004
0.2	3.07	150.0	0.016	2.52	150.0	0.011
0.3	4.37	150.0	0.026	3.15	150.0	0.017
0.4	6.13	150.0	0.039	4.24	150.0	0.025
0.5	8.05	150.0	0.052	5.30	150.0	0.033
0.6	10.69	150.0	0.070	6.90	150.0	0.044
0.7	14.00	150.0	0.093	8.63	150.0	0.056
0.8	20.06	150.0	0.133	12.20	150.0	0.080
0.9	22.92	150.0	0.152	14.30	150.0	0.095

Table 3. 150.0 GeV Incident Electrons - Renormalized Data

f	σ_p	E_p	B_p	σ_c	E_c	B_c
0.0	2.46	250.0	0.000	2.39	250.0	0.000
0.1	2.97	250.0	0.007	2.72	250.0	0.005
0.2	4.62	250.0	0.016	3.37	250.0	0.010
0.3	6.62	250.0	0.025	4.11	250.0	0.013
0.4	9.02	250.0	0.035	5.44	250.0	0.020
0.5	11.87	250.0	0.046	7.00	250.0	0.026
0.6	16.85	250.0	0.067	8.23	250.0	0.032
0.7	21.00	250.0	0.083	11.66	250.0	0.046
0.8	30.73	250.0	0.123	15.60	250.0	0.062
0.9	35.07	250.0	0.140	17.85	250.0	0.071

Table 4. 250.0 GeV Incident Electrons - Renormalized Data

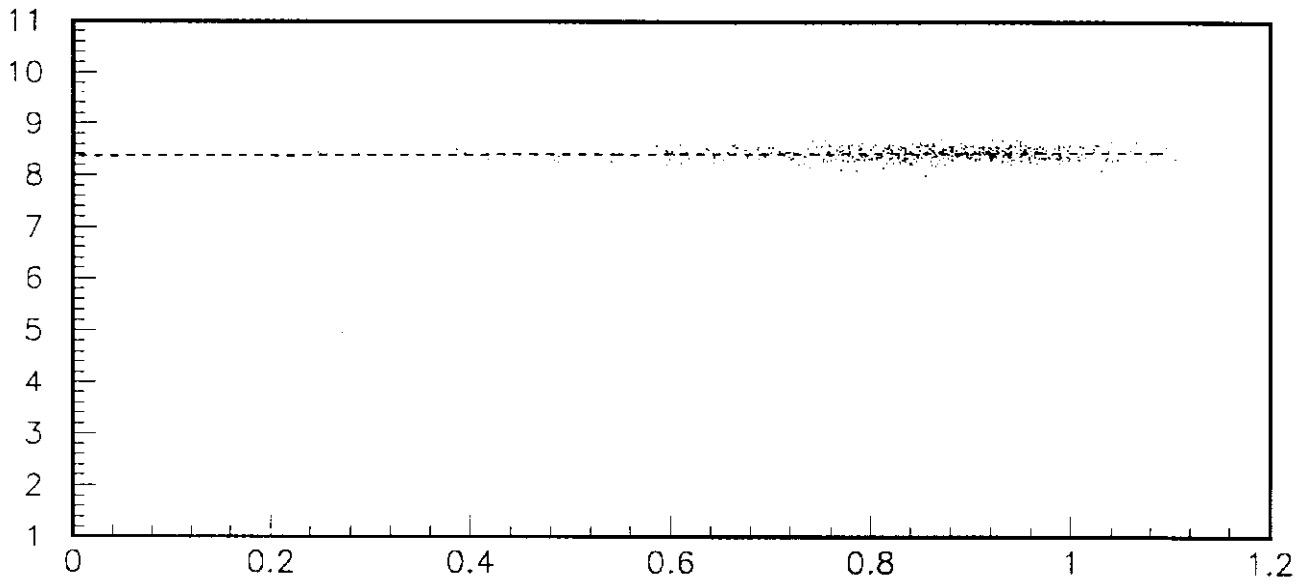
FIGURE CAPTIONS

1. Scatter plot of the total energy deposit (vertical axis) versus the energy deposit in the shower max detector (horizontal axis) together with histograms of the simple projection and fit residuals for 150 GeV incident electrons with $f = 0$.
2. Scatter plot of the total energy deposit (vertical axis) versus the energy deposit in the shower max detector (horizontal axis) together with histograms of the simple projection and fit residuals for 150 GeV incident electrons with $f = 0.1$.
3. Scatter plot of the total energy deposit (vertical axis) versus the energy deposit in the shower max detector (horizontal axis) together with histograms of the simple projection and fit residuals for 150 GeV incident electrons with $f = 0.2$.
4. Scatter plot of the total energy deposit (vertical axis) versus the energy deposit in the shower max detector (horizontal axis) together with histograms of the simple projection and fit residuals for 150 GeV incident electrons with $f = 0.3$.
5. Scatter plot of the total energy deposit (vertical axis) versus the energy deposit in the shower max detector (horizontal axis) together with histograms of the simple projection and fit residuals for 250 GeV incident electrons with $f = 0$.
6. Scatter plot of the total energy deposit (vertical axis) versus the energy deposit in the shower max detector (horizontal axis) together with histograms of the simple projection and fit residuals for 250 GeV incident electrons with $f = 0.1$.

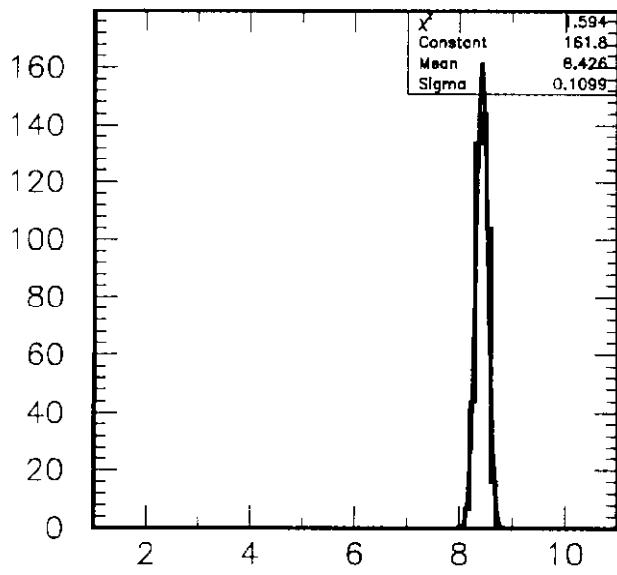
7. Scatter plot of the total energy deposit (vertical axis) versus the energy deposit in the shower max detector (horizontal axis) together with histograms of the simple projection and fit residuals for 250 GeV incident electrons with $f = 0.2$.
8. Scatter plot of the total energy deposit (vertical axis) versus the energy deposit in the shower max detector (horizontal axis) together with histograms of the simple projection and fit residuals for 250 GeV incident electrons with $f = 0.3$.
9. Scatter plot of the rescaled total energy deposit (vertical axis) versus the energy deposit in the shower max detector (horizontal axis) together with histograms of the simple projection and fit residuals for 150 GeV incident electrons with $f = 0.1$.
10. Scatter plot of the rescaled total energy deposit (vertical axis) versus the energy deposit in the shower max detector (horizontal axis) together with histograms of the simple projection and fit residuals for 150 GeV incident electrons with $f = 0.2$.
11. Scatter plot of the rescaled total energy deposit (vertical axis) versus the energy deposit in the shower max detector (horizontal axis) together with histograms of the simple projection and fit residuals for 150 GeV incident electrons with $f = 0.3$.
12. Scatter plot of the rescaled total energy deposit (vertical axis) versus the energy deposit in the shower max detector (horizontal axis) together with histograms of the simple projection and fit residuals for 250 GeV incident electrons with $f = 0.1$.
13. Scatter plot of the rescaled total energy deposit (vertical axis) versus the energy deposit in the shower max detector (horizontal axis) together with histograms of the simple projection and fit residuals for 250 GeV incident electrons with $f = 0.2$.

14. Scatter plot of the rescaled total energy deposit (vertical axis) versus the energy deposit in the shower max detector (horizontal axis) together with histograms of the simple projection and fit residuals for 250 GeV incident electrons with $f = 0.3$.
15. B_p and B_c as functions of f for the 150 GeV data. The curves shown only serve to organize the results and do not represent a meaningful fit.
16. B_p and B_c as functions of f for the 250 GeV data. The curves shown only serve to organize the results and do not represent a meaningful fit.

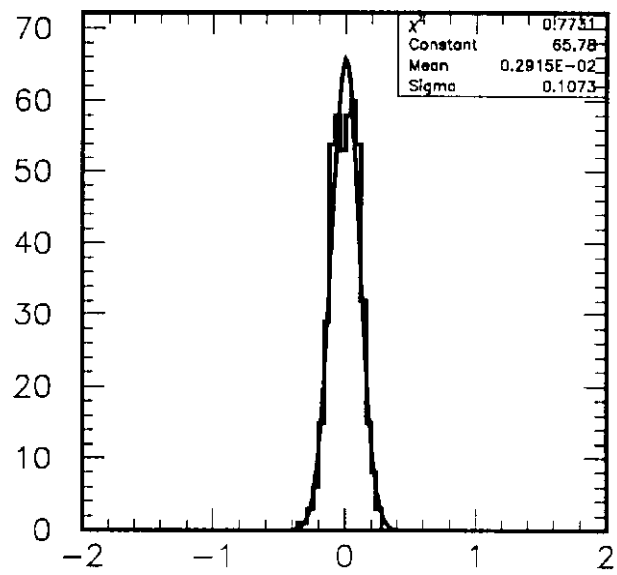
Electron Energy = 150 GeV
Damage Fraction = 00 per cent



Total Energy Deposit vs Shower Max Energy Deposit (GeV)



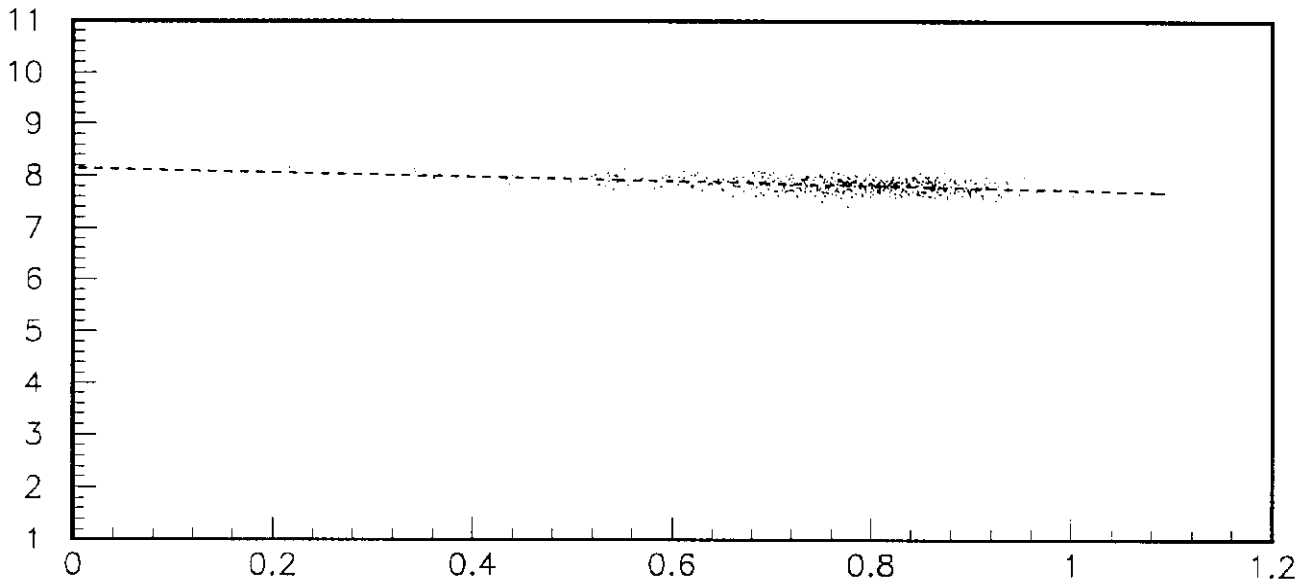
Total Energy Deposit (GeV)



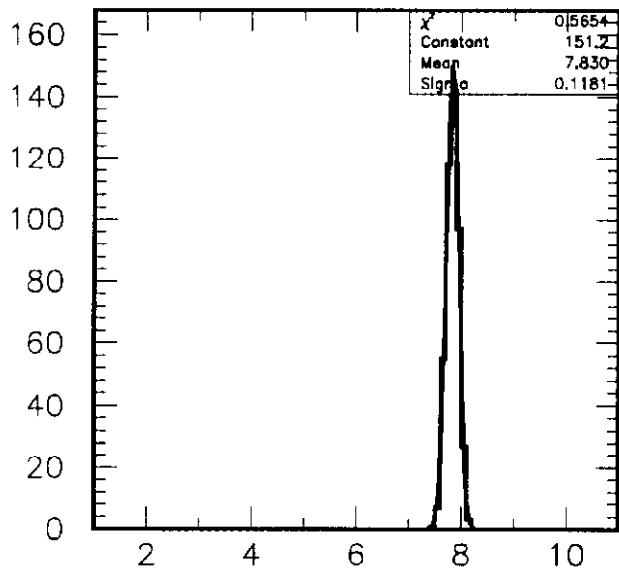
Fit Residuals

Figure 1

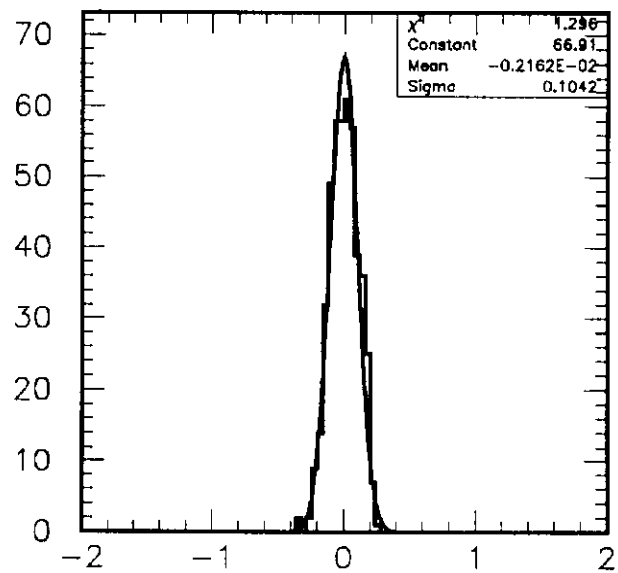
Electron Energy = 150 GeV
Damage Fraction = 10 per cent



Total Energy Deposit vs Shower Max Energy Deposit (GeV)



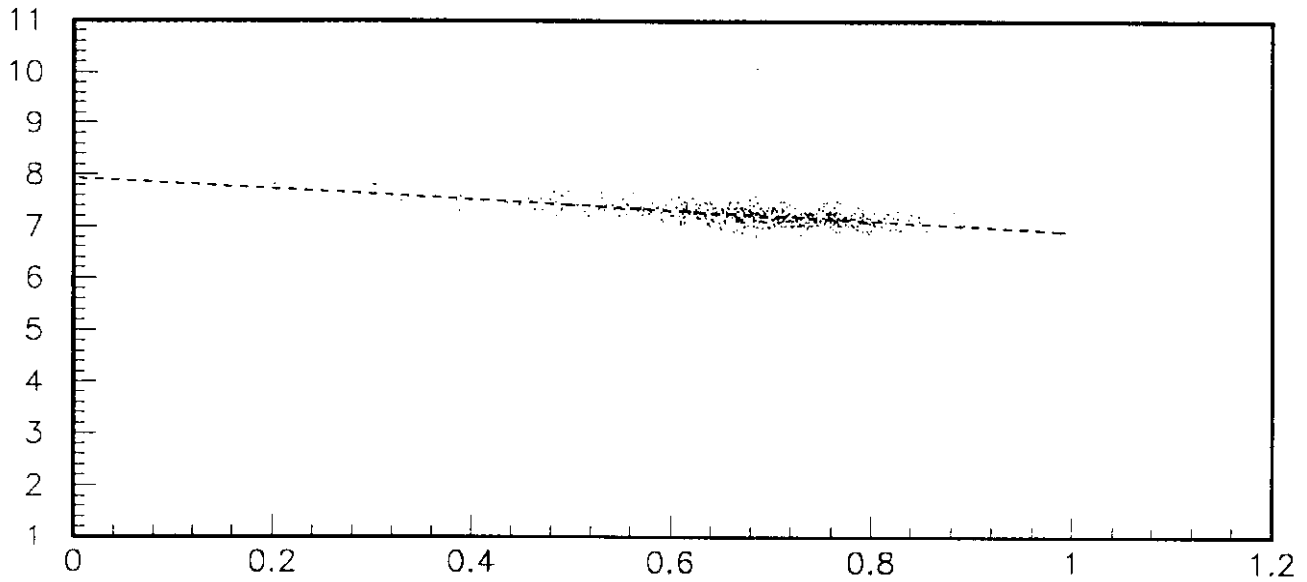
Total Energy Deposit (GeV)



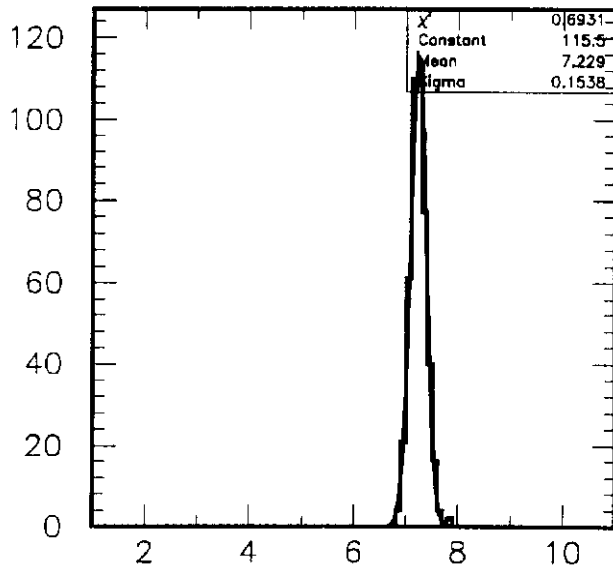
Fit Residuals

Figure 2

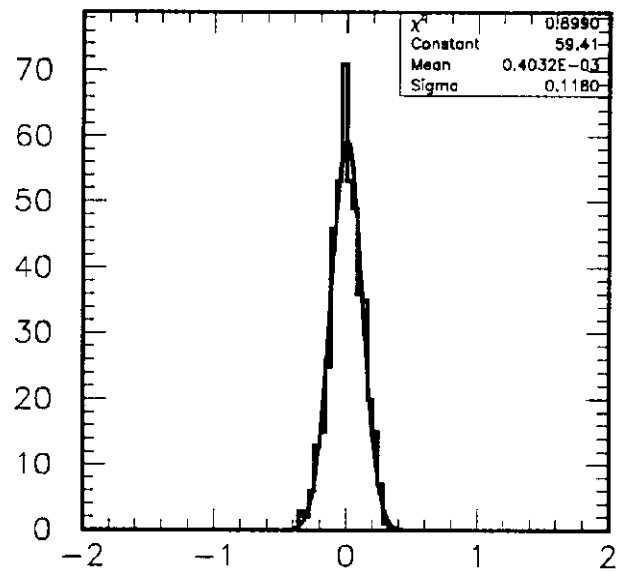
Electron Energy = 150 GeV
Damage Fraction = 20 per cent



Total Energy Deposit vs Shower Max Energy Deposit (GeV)



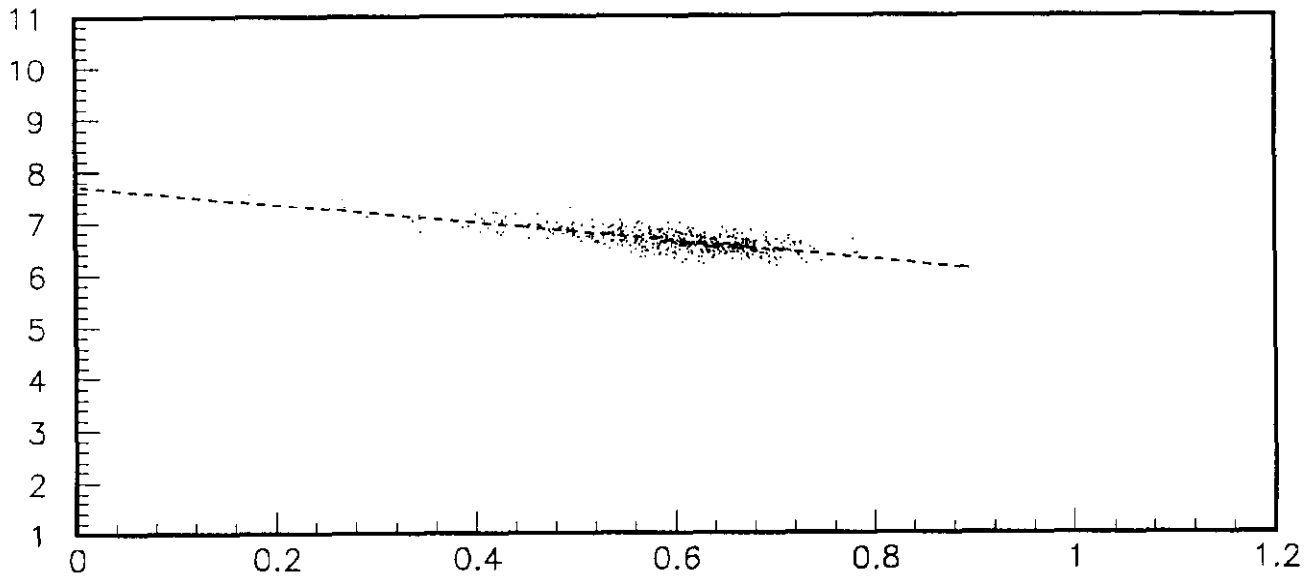
Total Energy Deposit (GeV)



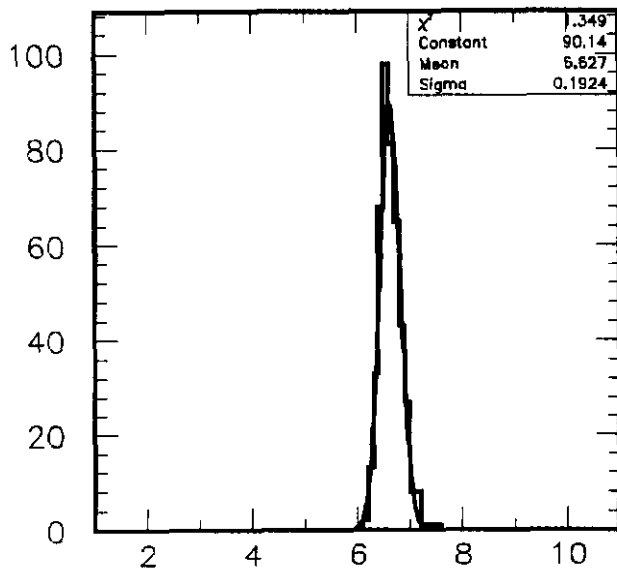
Fit Residuals

Figure 3

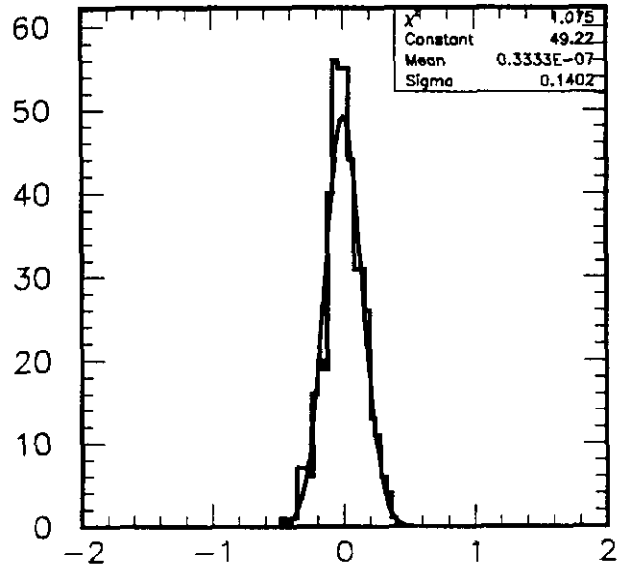
Electron Energy = 150 GeV
Damage Fraction = 30 per cent



Total Energy Deposit vs Shower Max Energy Deposit (GeV)



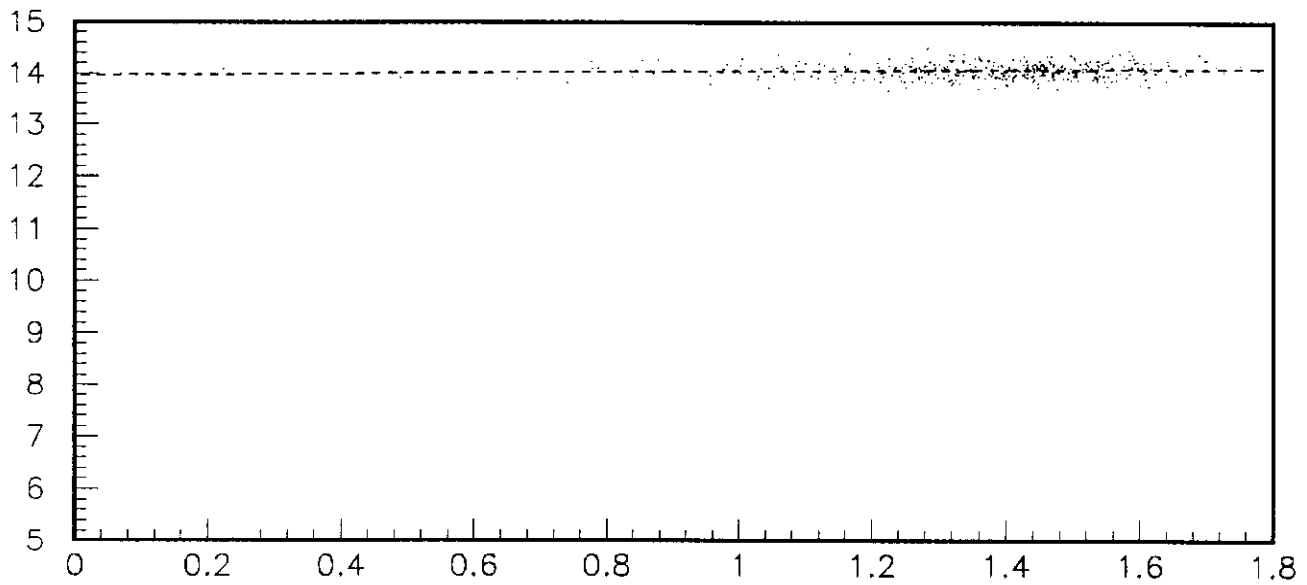
Total Energy Deposit (GeV)



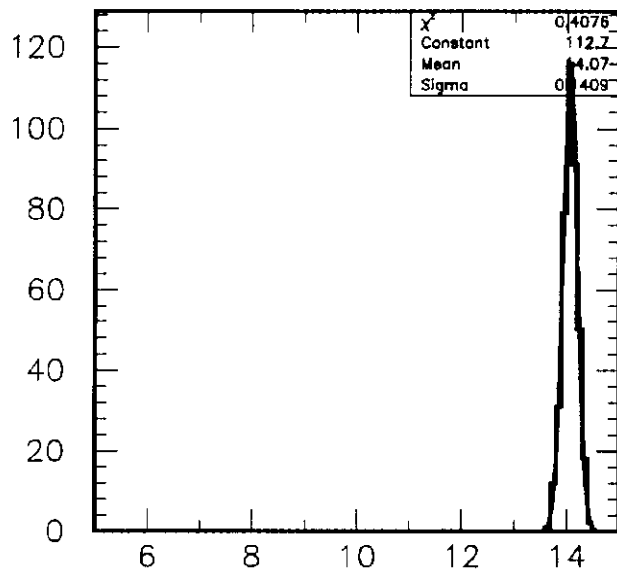
Fit Residuals

Figure 4

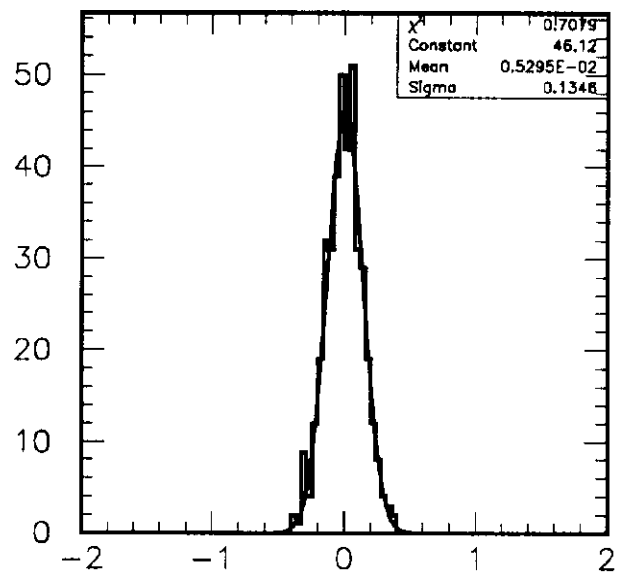
Electron Energy = 250 GeV
Damage Fraction = 00 per cent



Total Energy Deposit vs Shower Max Energy Deposit (GeV)



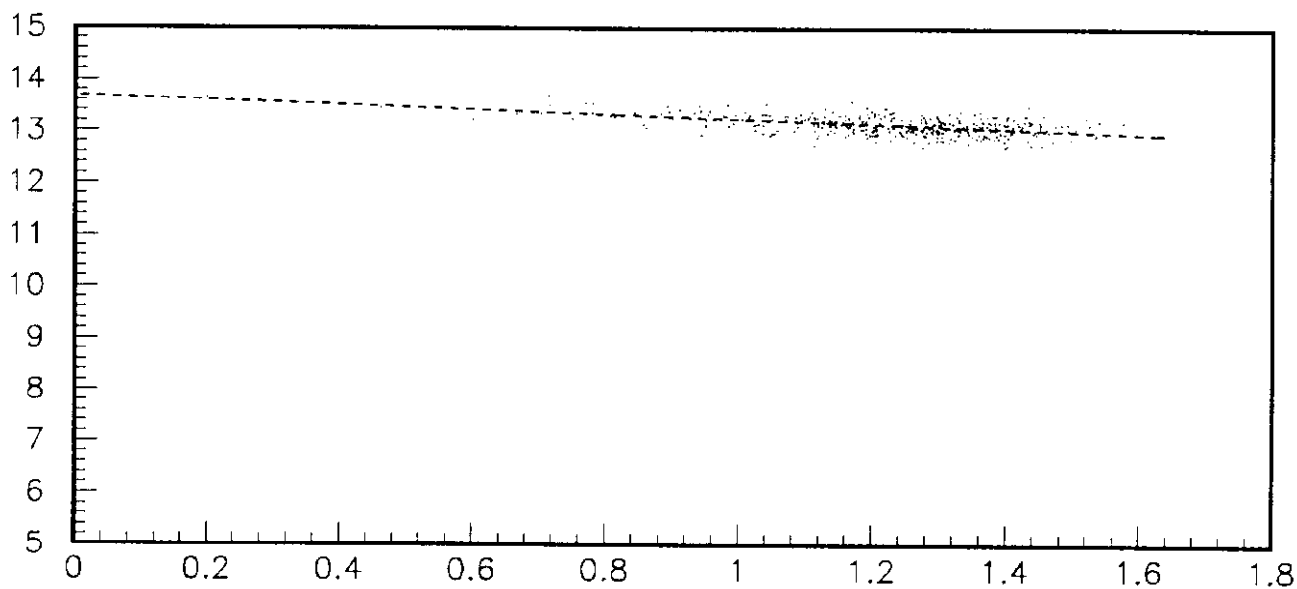
Total Energy Deposit (GeV)



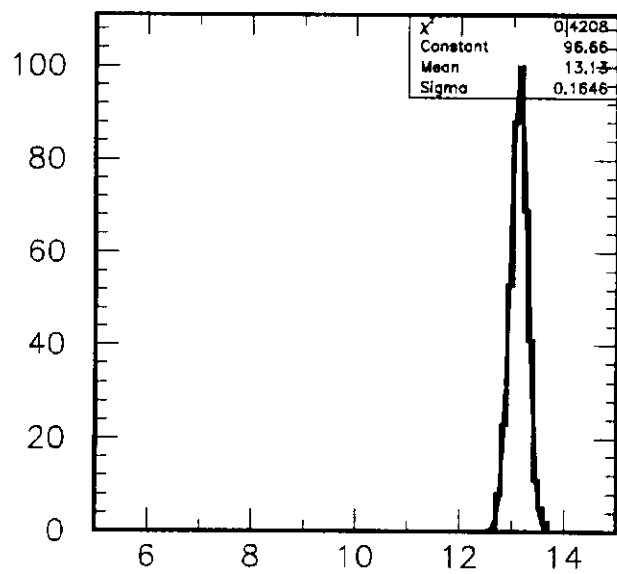
Fit Residuals

Figure 5

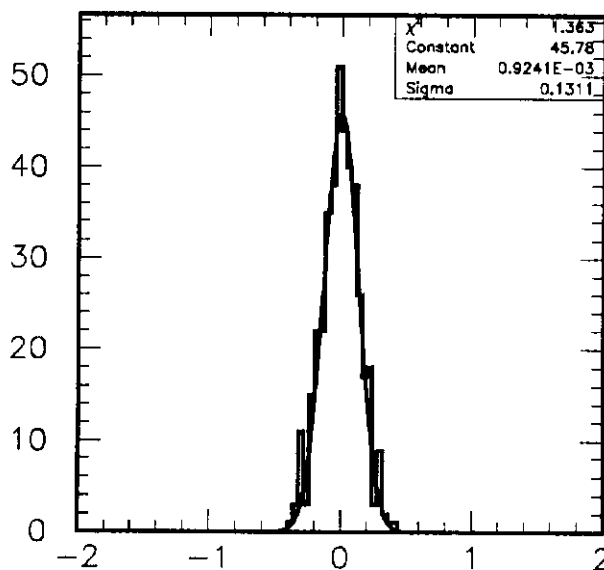
Electron Energy = 250 GeV
Damage Fraction = 10 per cent



Total Energy Deposit vs Shower Max Energy Deposit (GeV)



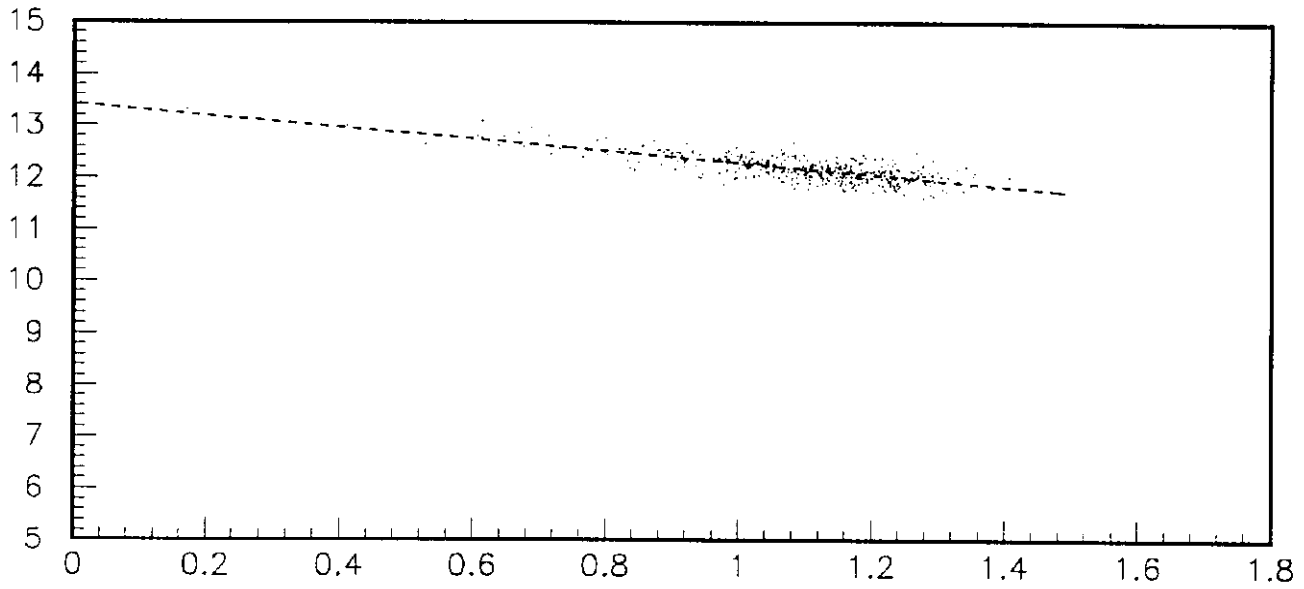
Total Energy Deposit (GeV)



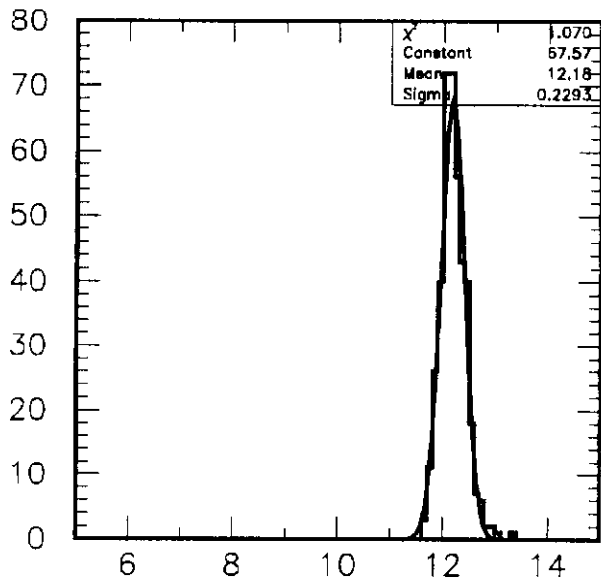
Fit Residuals

Figure 6

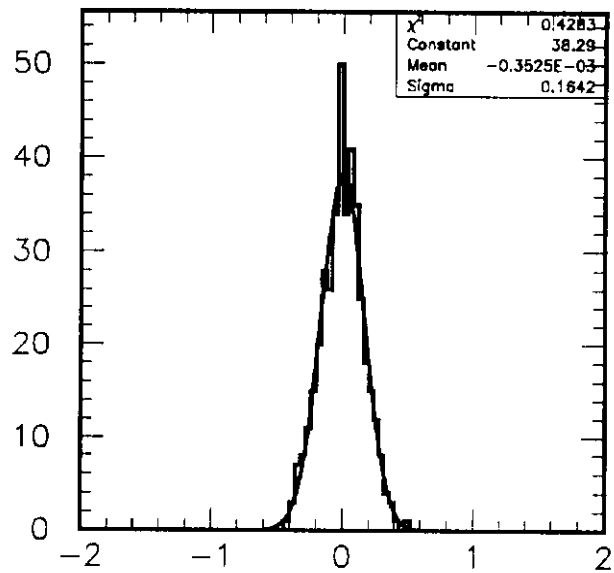
Electron Energy = 250 GeV
Damage Fraction = 20 per cent



Total Energy Deposit vs Shower Max Energy Deposit (GeV)



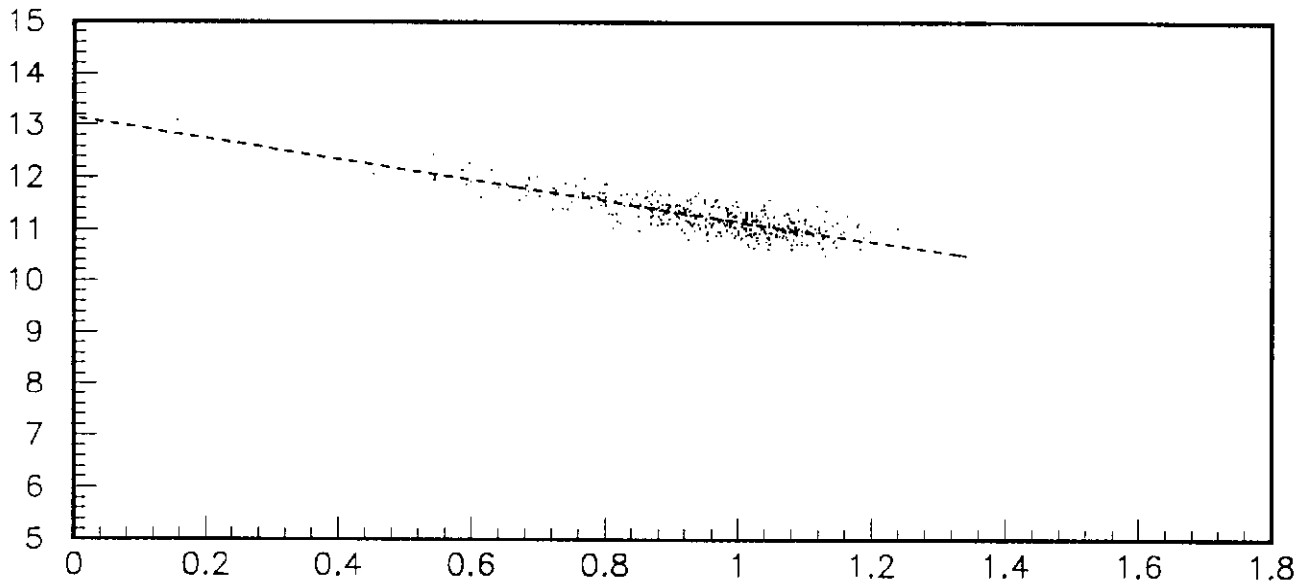
Total Energy Deposit (GeV)



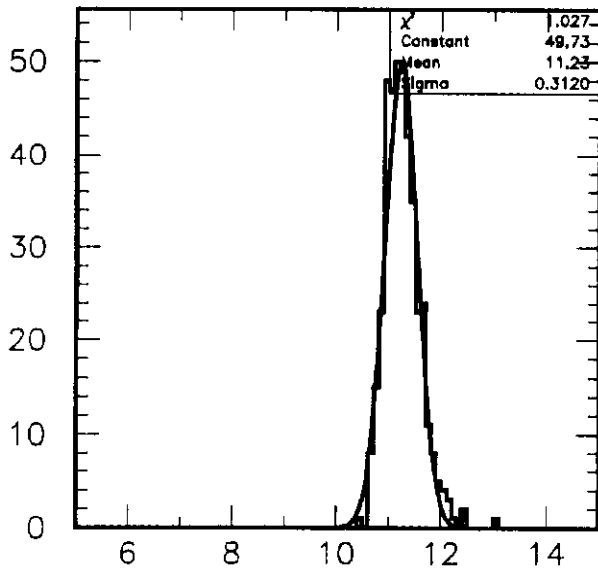
Fit Residuals

Figure 7

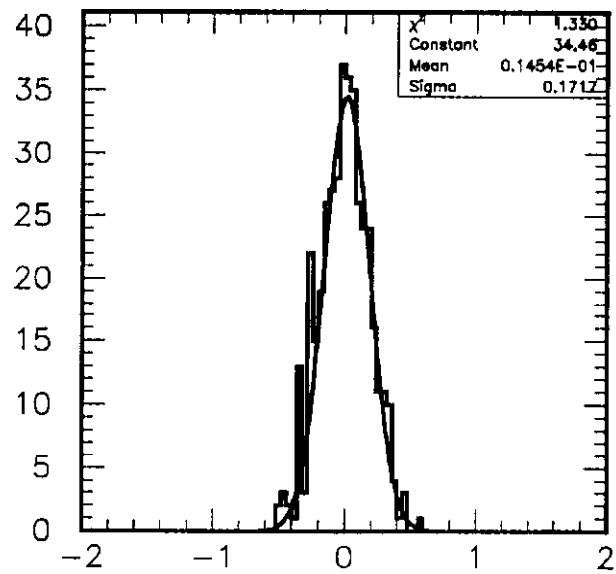
Electron Energy = 250 GeV
Damage Fraction = 30 per cent



Total Energy Deposit vs Shower Max Energy Deposit (GeV)



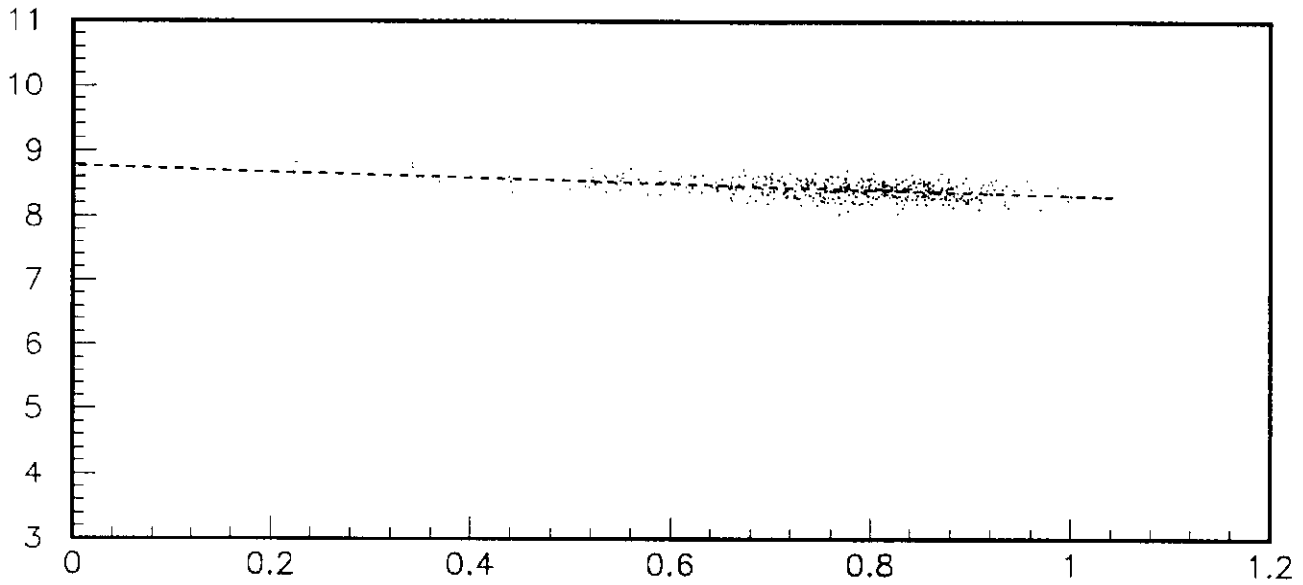
Total Energy Deposit (GeV)



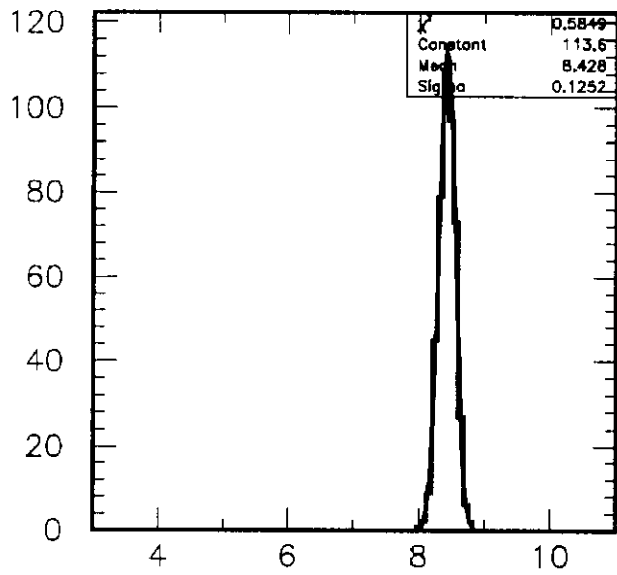
Fit Residuals

Figure 8

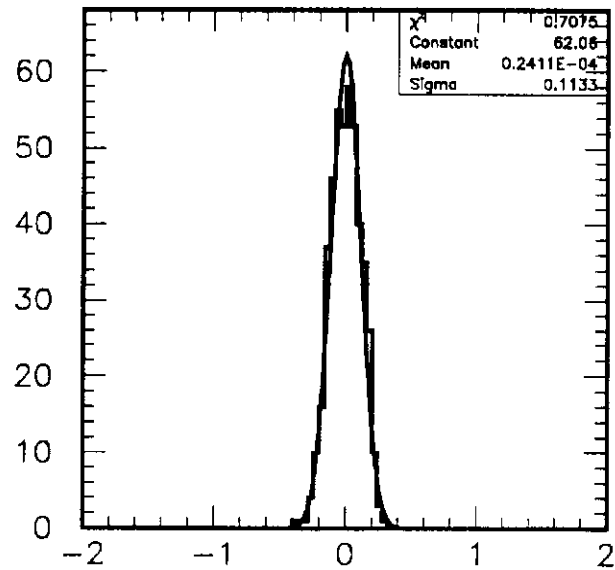
Electron Energy = 150 GeV
Damage Fraction = 10 per cent



Rescaled Total Energy Deposit vs Shower Max Energy Deposit (GeV)



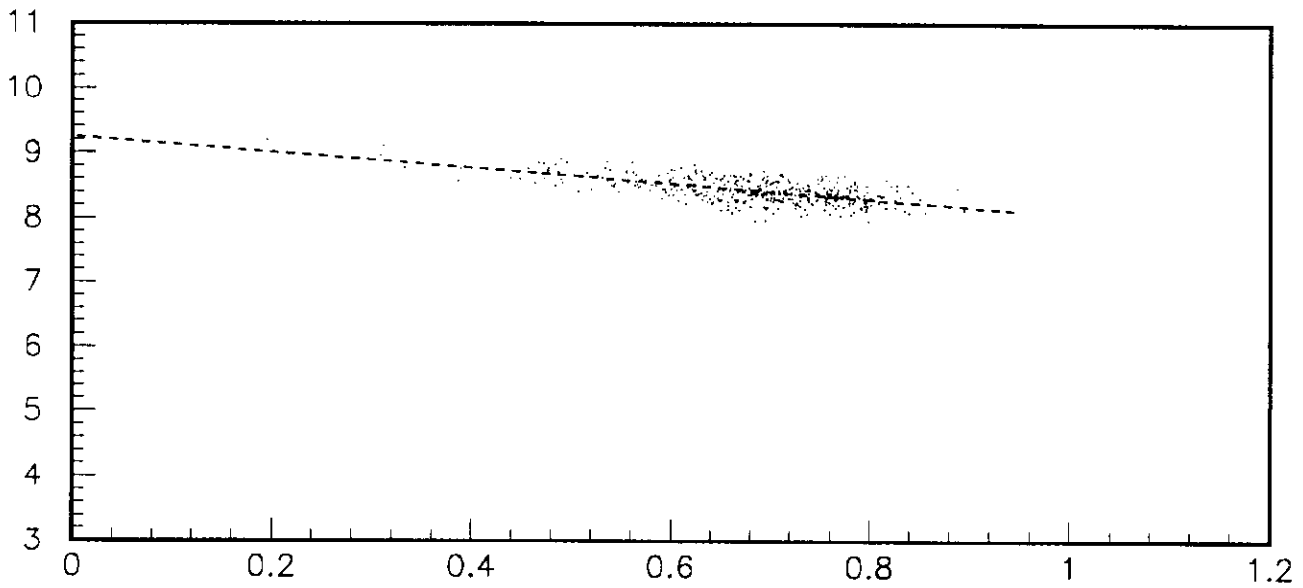
Rescaled Energy Deposit (GeV)



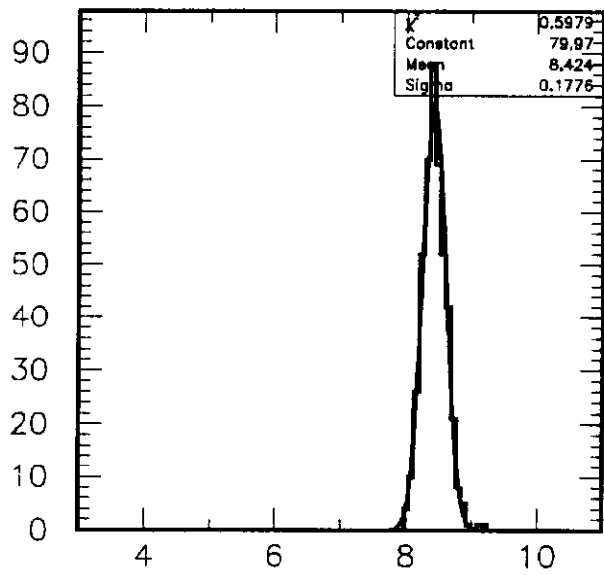
Fit Residuals

Figure 9

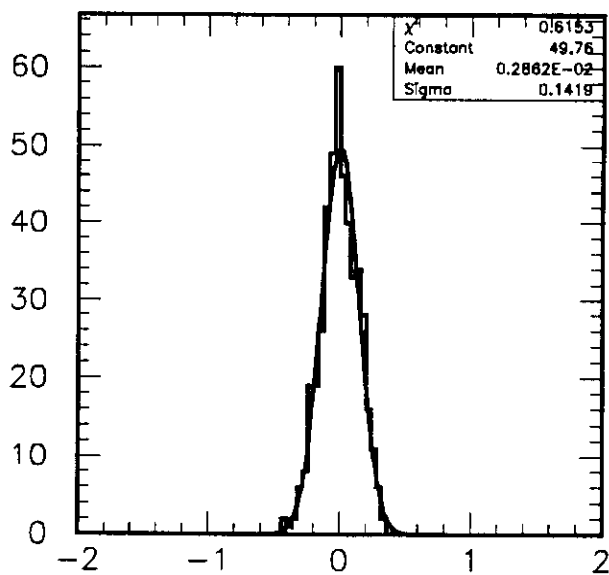
Electron Energy = 150 GeV
Damage Fraction = 20 per cent



Rescaled Total Energy Deposit vs Shower Max Energy Deposit (GeV)



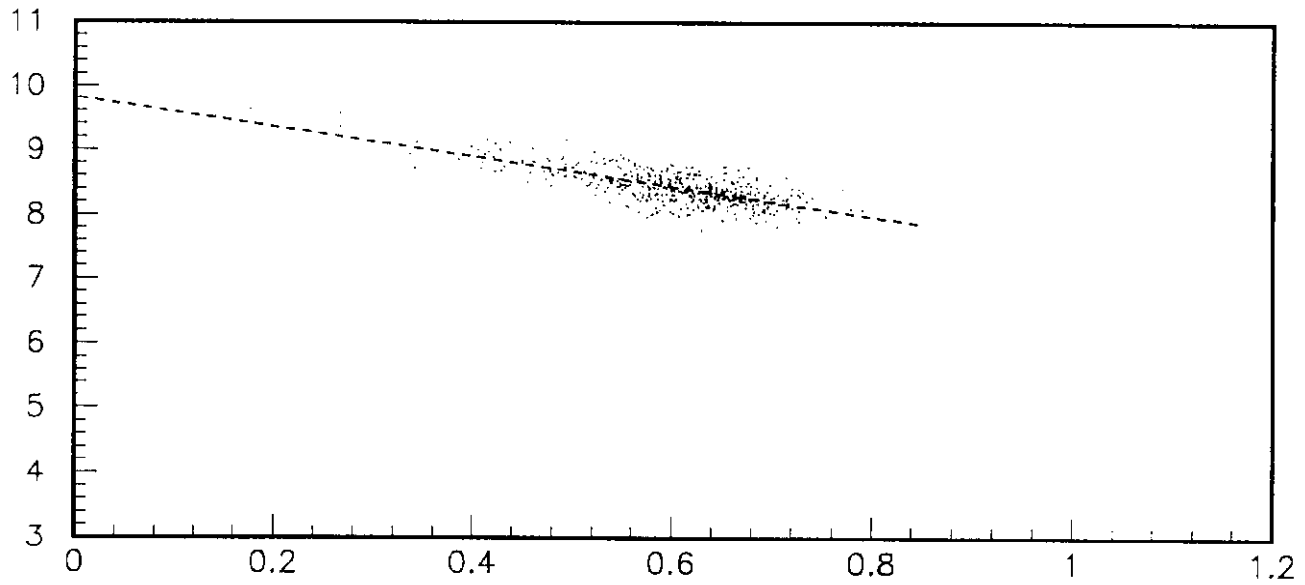
Rescaled Energy Deposit (GeV)



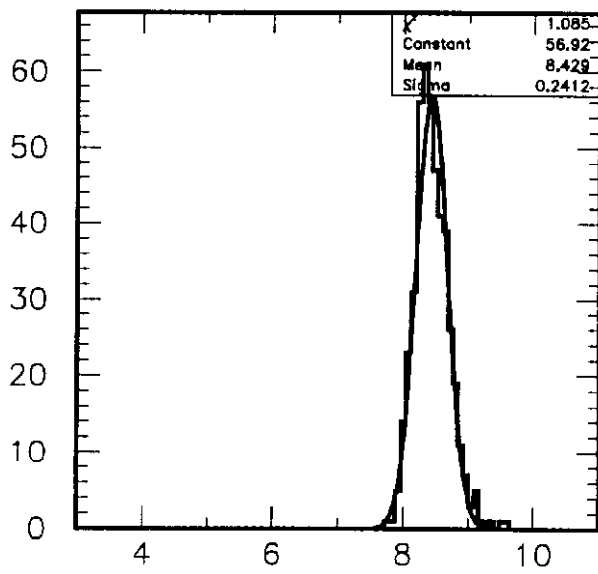
Fit Residuals

Figure 10

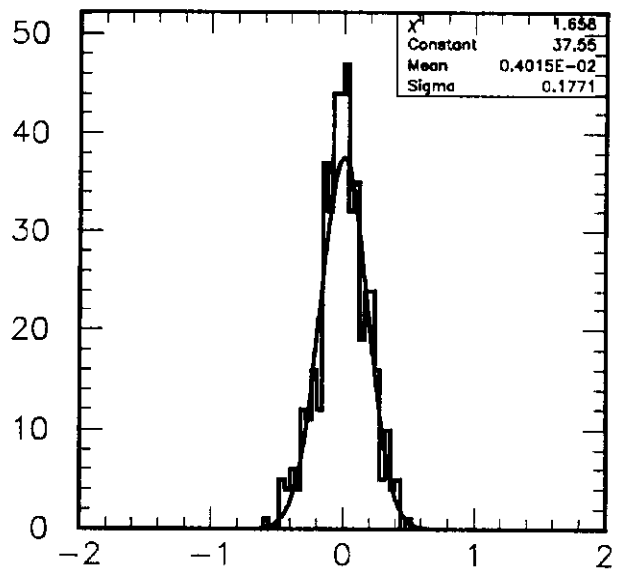
Electron Energy = 150 GeV
Damage Fraction = 30 per cent



Rescaled Total Energy Deposit vs Shower Max Energy Deposit (GeV)



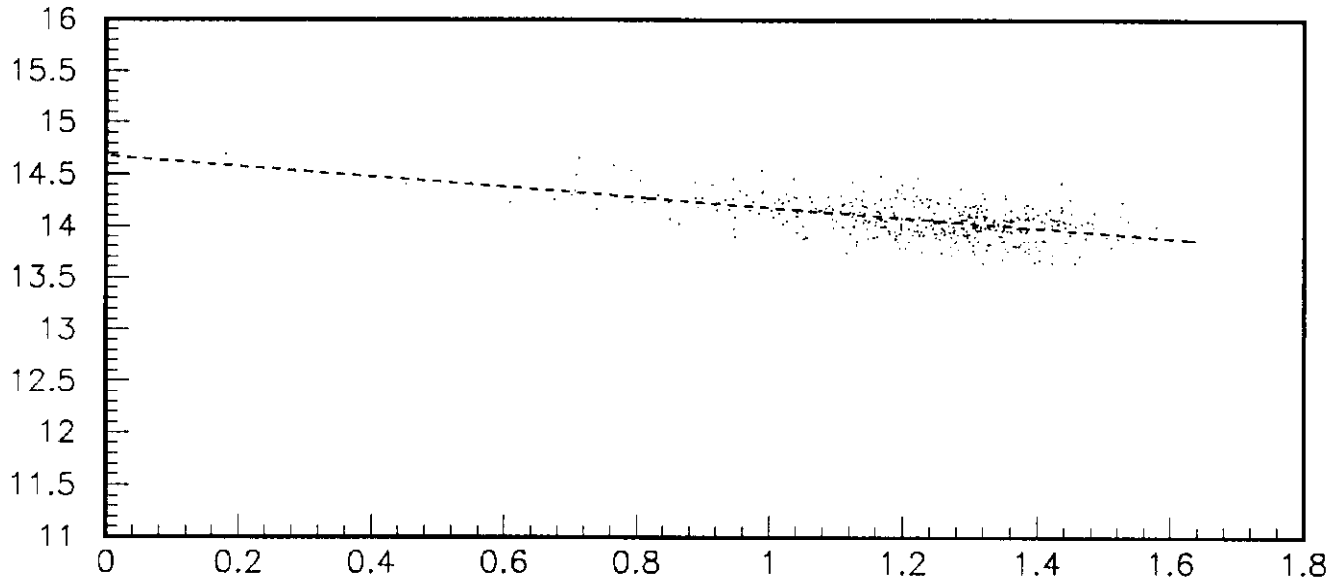
Rescaled Energy Deposit (GeV)



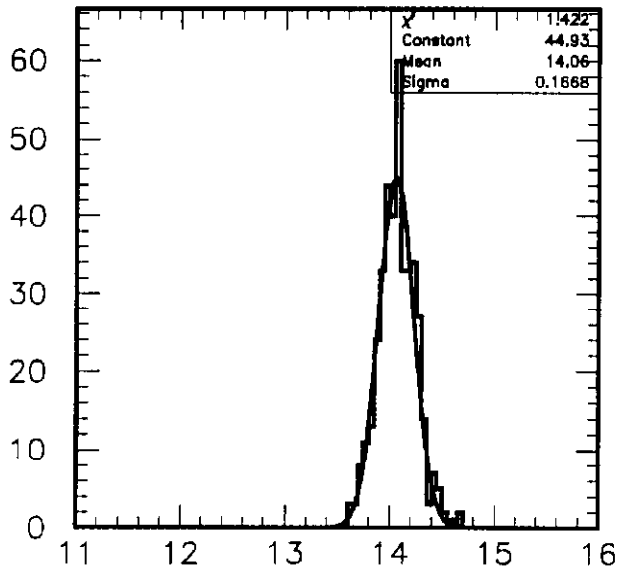
Fit Residuals

Figure 11

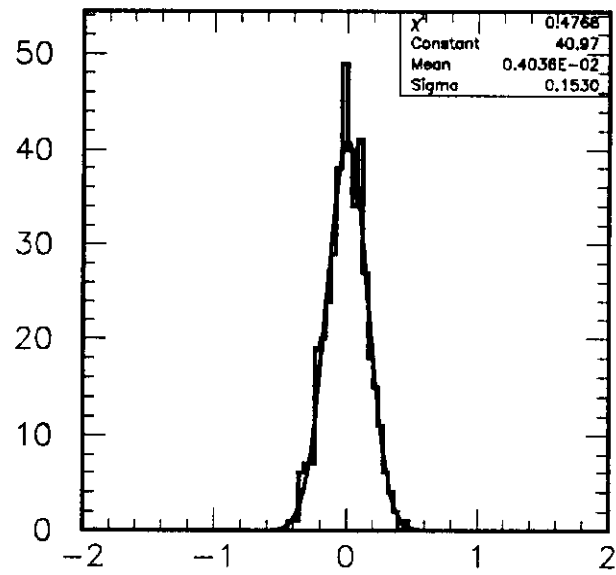
Electron Energy = 250 GeV
Damage Fraction = 10 per cent



Rescaled Total Energy Deposit vs Shower Max Energy Deposit (GeV)



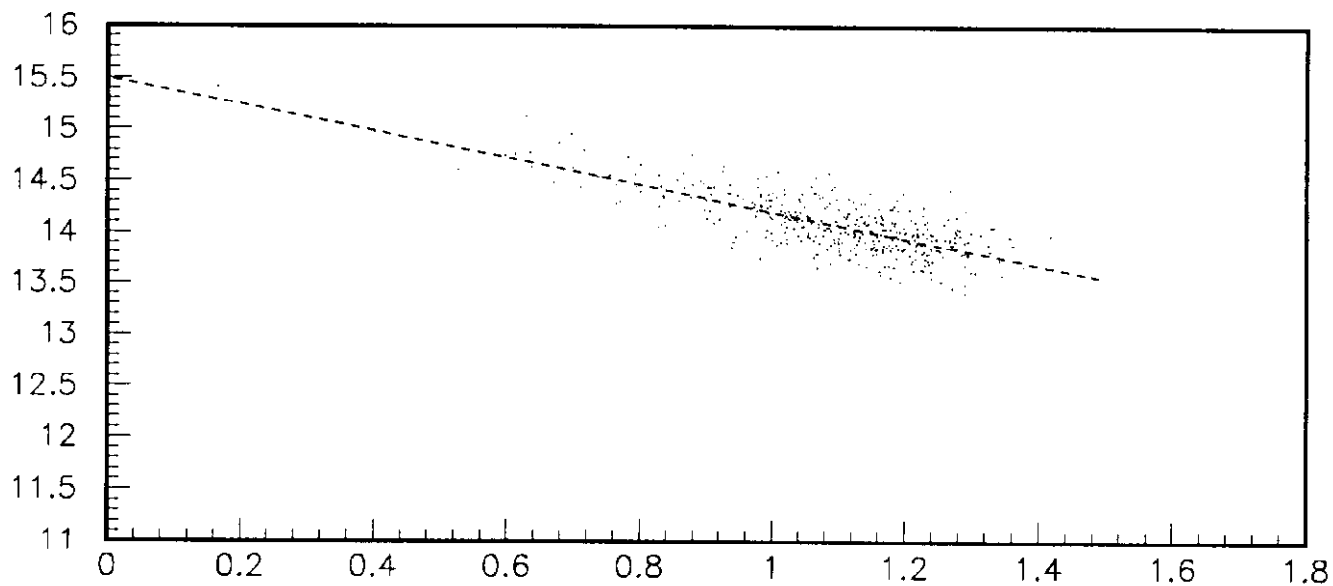
Rescaled Energy Deposit (GeV)



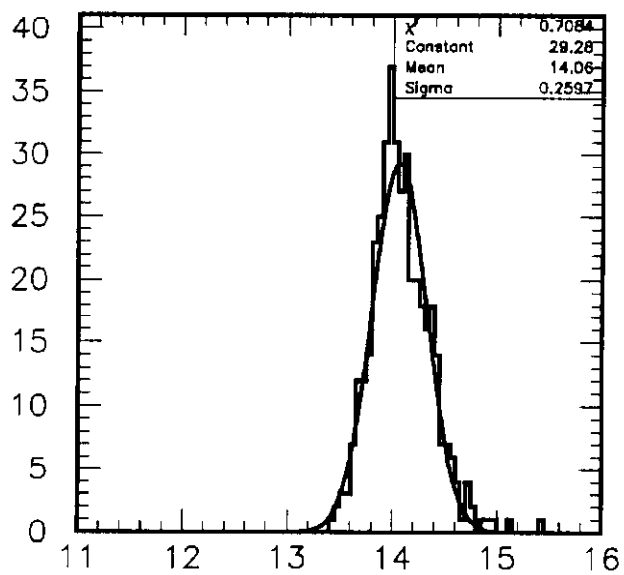
Fit Residuals

Figure 12

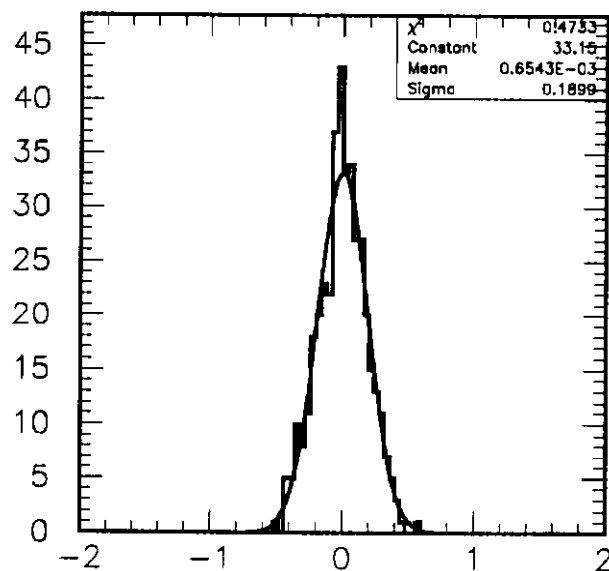
Electron Energy = 250 GeV
Damage Fraction = 20 per cent



Rescaled Total Energy Deposit vs Shower Max Energy Deposit (GeV)



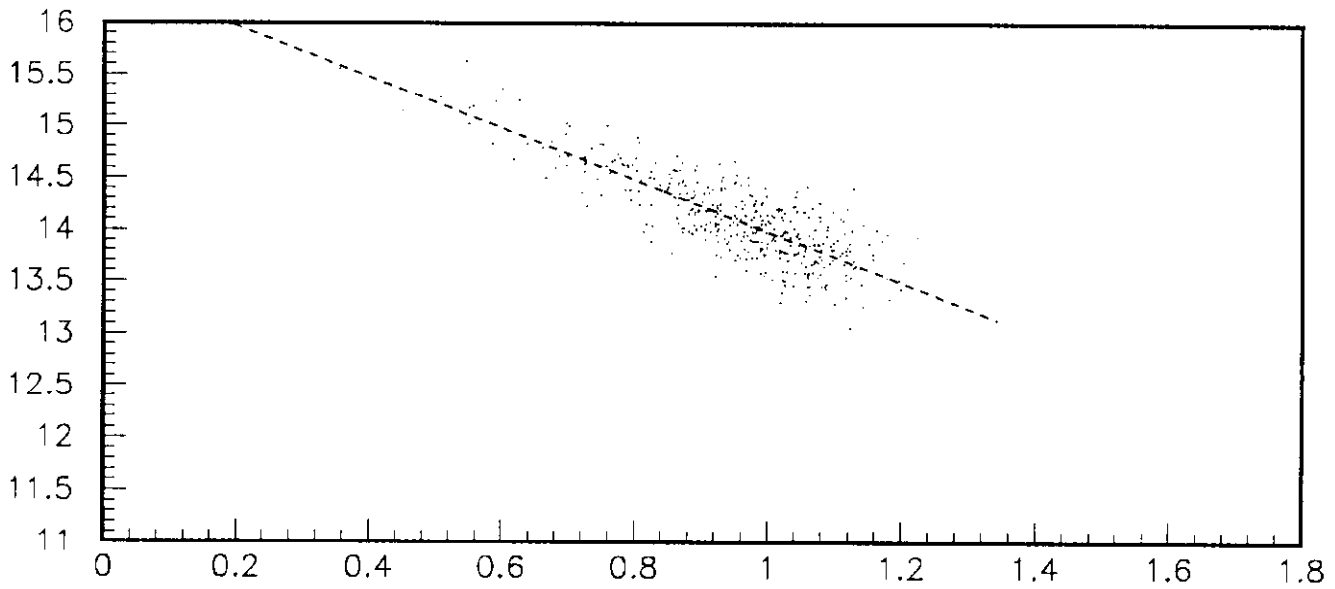
Rescaled Energy Deposit (GeV)



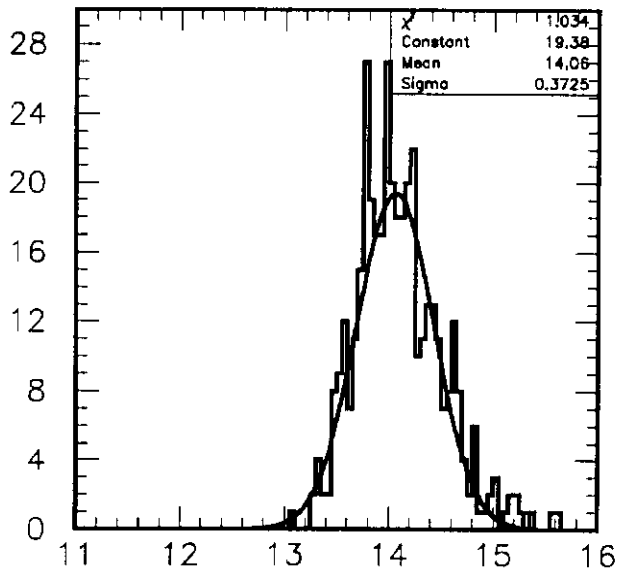
Fit Residuals

Figure 13

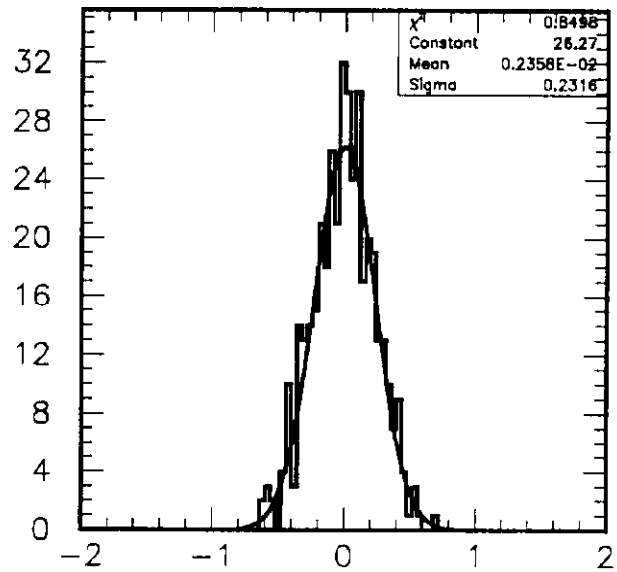
Electron Energy = 250 GeV
Damage Fraction = 30 per cent



Rescaled Total Energy Deposit vs Shower Max Energy Deposit (GeV)



Rescaled Energy Deposit (GeV)



Fit Residuals

Figure 14

Electron Energy = 150 GeV

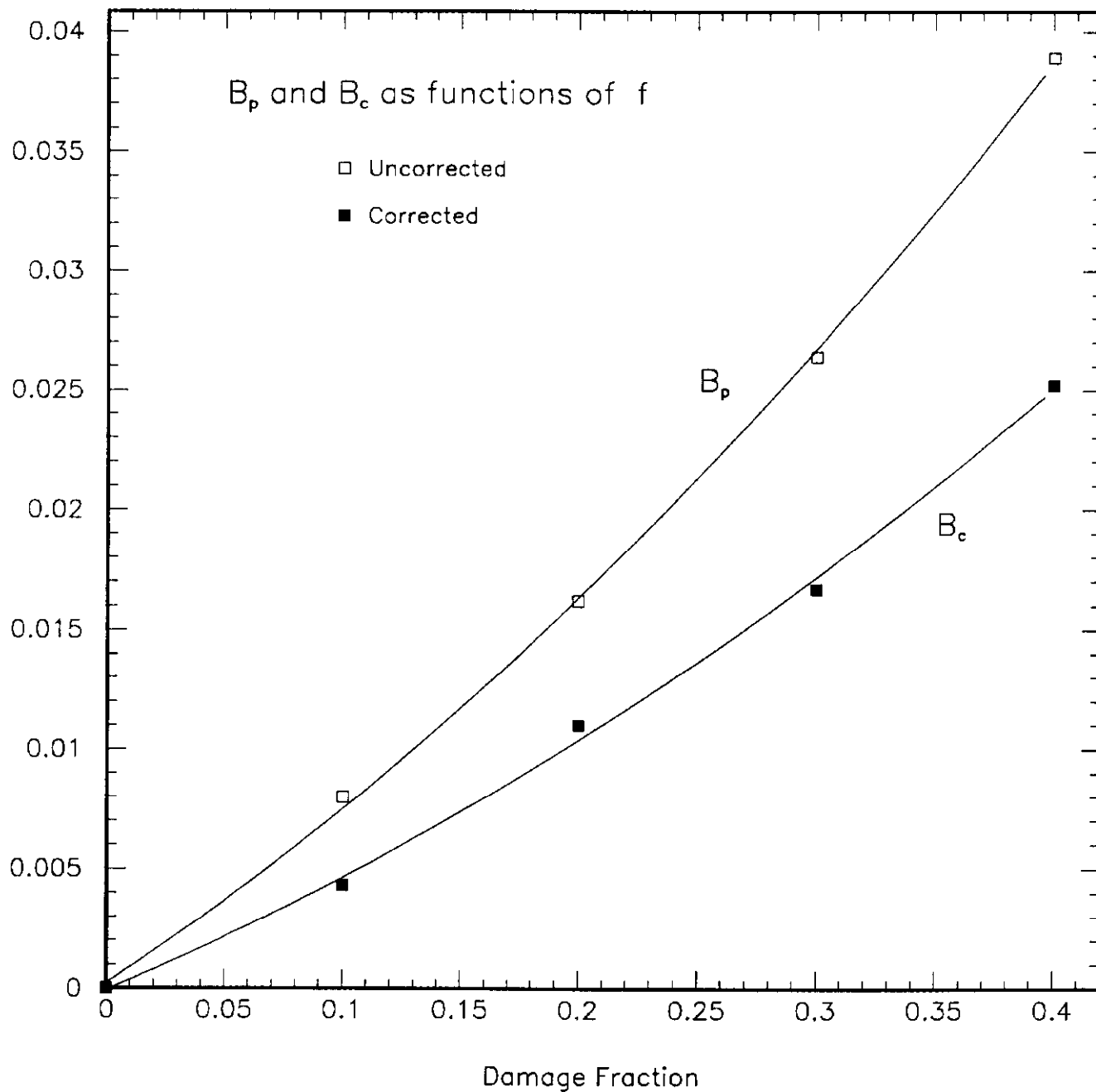


Figure 15

Electron Energy = 250 GeV

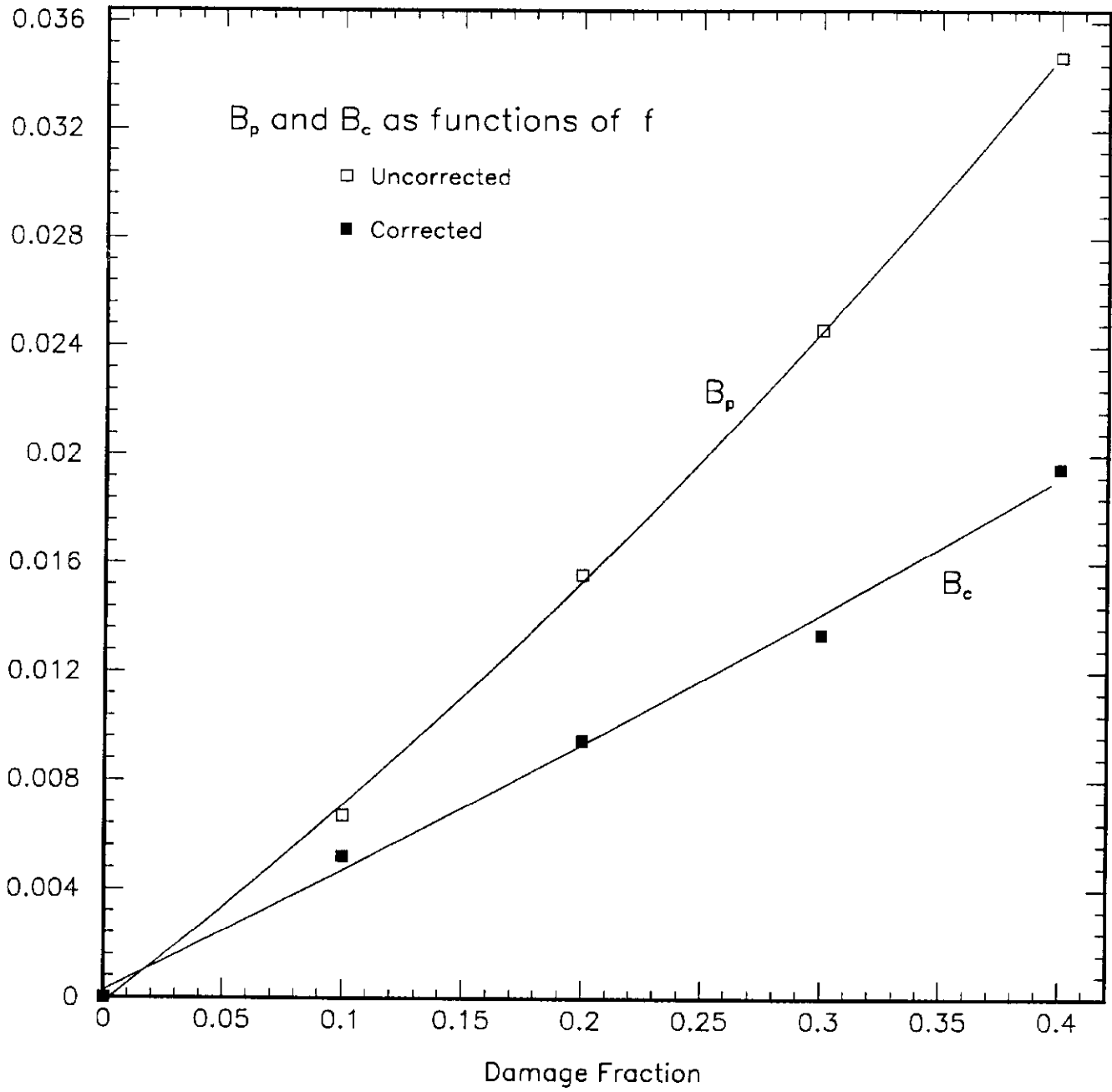


Figure 16